2023 IEEE International Conference on Robotics and Automation (ICRA 2023)
May 29 - June 2, 2023. London, UK

A method for selecting stumble recovery response in a knee exoskeleton

Maura Eveld[1,2], Shane King[1], Karl Zelik[1], Michael Goldfarb[1], *Member, IEEE*

***Abstract*— Powered lower-limb exoskeletons have been shown to assist and augment walking, but most such devices do not currently have the ability to explicitly accommodate a stumble perturbation. A major challenge in doing so is identifying a stumble event and selecting in real-time which recovery strategy (elevating or lowering) to employ, particularly since the exoskeleton should ideally select the same strategy selected by the user. In order to do so, the authors conducted experiments involving five young, healthy adults wearing a knee exoskeleton. Each participant underwent a stumble experiment in order to collect an exoskeleton sensor dataset of stumbles throughout swing phase, which was used for stumble detection and recovery strategy identification algorithm development and testing. Overall, the proposed detection and identification algorithms provide improved accuracy with fewer required sensors relative to previous works, and were tested on the largest exoskeleton sensor stumble dataset to date, showing the feasibility of such algorithms for real-time implementation, which is an essential first step in developing lower-limb assistive devices that are robust to stumbles.**

I. INTRODUCTION

Powered lower-limb exoskeletons show promise as rehabilitation devices for walking-impaired users (e.g., [1]) and as performance augmentation devices for healthy users (e.g., [2]). However, for such devices to be safe and ultimately adopted in the real world, their function should be robust to unexpected perturbations, such as a trip or stumble [3], [4], [5], [6].

The response of healthy adults to stumbles (i.e., the event in which the swing foot unexpectedly encounters an obstacle and must navigate up and over, or clear, that obstacle to recover) has been relatively well characterized, offering insights into how a lower-limb exoskeleton might behave. Upon contact with an obstacle, the healthy adult reacts with biceps femoris or rectus femoris response latencies of about 60 ms (among other muscle responses) [7]. These muscle responses commence one of three primary recovery strategies: the elevating, lowering, or delayed lowering strategy [8], [7]. In the elevating strategy, the tripped limb elevates up and over the obstacle, clearing the obstacle in the same step. In the lowering strategy, the tripped limb lowers to the ground posterior to the obstacle, prematurely terminating the step, and the contralateral limb subsequently completes a recovery step; the tripped limb then clears the obstacle in the following step. In the delayed lowering strategy, the tripped limb initially elevates, but ultimately elevation is abandoned and the limb is lowered posterior to the obstacle akin to the lowering strategy. Note that the elevating strategy is characterized by tripped limb knee and hip flexion (to elevate over the obstacle), while the lowering and delayed lowering strategies are characterized by tripped limb knee and hip extension (to terminate the step posterior to the obstacle).

Thus, in order to provide appropriate stumble recovery assistance, a lower-limb exoskeleton ideally would have the following behaviors: (i) the reliable and quick detection of a swing-phase perturbation and (ii) the correct recovery strategy decision (i.e., elevating or lowering). Regarding (i), studies have taken various approaches to investigate potential stumble detection algorithms for powered lower-limb assistive devices, which have provided meaningful insights for this work. Zhang et al. 2011 [9] used anterior-posterior foot acceleration from motion capture data and lower-limb electromyography (EMG) data to detect perturbations; while they achieved high detection accuracy, they reported that further research is needed to improve the false positive rate and detection response time. Additionally, their perturbation study involved treadmill belt accelerations and decelerations (rather than swing-phase obstacle perturbations) which may not accurately represent real-life stumbles [10]; moreover, using motion capture and EMG data may not be representative of sensor data for assistive device applications. Shirota et al. 2014 [11] considered tripped limb kinematics from motion capture data in their linear discriminant analysis classifier when participants were tripped via a rope-blocking apparatus on a treadmill. While all stumbles were detected, the authors also encouraged further research to decrease false positives. Lawson et al. 2010 [12] used a Fast Fourier Transform (FFT) approach to detect stumbles from participants wearing IMUs during overground obstacle perturbations, which yielded 100% accuracy with a 50 ms detection delay and no false positives. However, three inertial measurement units (IMUs) were employed on three leg segments, which may not be available in some lower-limb devices. Furthermore, a larger test set (19 stumbles were included in this work) would give a better indication of efficacy. Monaco et al. 2017 [13] detected balance loss during treadmill belt acceleration perturbations when participants were wearing a powered hip exoskeleton by comparing actual hip angle to those predicted by a pool of adaptive oscillators with an average detection delay of 350 ms, which is much longer than that observed in the healthy human response (e.g., [7]). A few other studies have explored stumble detection with a single IMU during obstacle perturbations and achieved high detection accuracy [14], [15]; however, these algorithms were intended for more clinical applications analyzing patient stumble rate over an extended period of time, and as such do not detect quick

*This work was supported by NIH and NSF
[1]Department of Mechanical Engineering, Vanderbilt University, Nashville, TN 37209 USA
[2]maura.e.eveld@vanderbilt.edu

enough for real-time exoskeleton assistance.

Regarding (ii) – making the correct recovery decision – only two studies have specifically investigated the development of a real-time stumble recovery strategy selection algorithm for lower-limb wearable assistive devices, which have given important direction for this work. Shirota et al. 2014 [11] used a linear discriminant analysis classifier to classify elevating or lowering strategies and achieved 92% median classification accuracy. The algorithm, however, used motion capture kinematics from multiple joints/segments, which limits real-world use in an assistive device. Additionally, the rope-blocking perturbation technique does not involve a physical obstacle to clear, which may alter recovery strategy selection compared to real-life stumbles. Lawson et al. [12] found a threshold on the RMS of thigh acceleration 50 ms prior to detection that separated elevating from lowering strategies. However, their overground stumble apparatus limited the ability to implement stumbles across swing phase, and therefore it is unclear if mid swing stumbles were tested. Additionally, further testing with more stumbles (19 were tested in this work) would provide a more complete validation of this approach.

Considering these previous works, a stumble detection algorithm and stumble recovery identification algorithm that (1) use sensors typical of a lower-limb exoskeleton, (2) detect a stumble and select an anticipated recovery strategy within the human muscle response latency for stumbles, (3) offer high stumble detection accuracy and recovery strategy identification classification accuracy without false positives, and (4) are tested on many (more than 20) swing-phase obstacle perturbations (i.e., real-life stumbles) throughout swing phase would build upon prior research and address the problem in a manner that is closer to real-world application.

The authors have previously developed a stumble detection algorithm and recovery strategy identification algorithm for a knee exoskeleton that was evaluated on one healthy adult [16]. The detection algorithm used a simple threshold on thigh acceleration. The recovery strategy identification algorithm implemented a two-stage decision model with logistic regression equations fit from previously collected healthy adult motion capture stumble data [17]. While these approaches yielded 100% detection and classification accuracy for the single participant, the extent to which these approaches might extend across multiple participants has not been tested and is critical for robustness analysis and implementation in the real world. Therefore, the objective of this work is to develop and test a new stumble detection algorithm and recovery strategy identification algorithm with the aforementioned criteria using experimental stumble data from multiple healthy adults wearing a knee exoskeleton.

II. METHODS

The following approach was taken to address the proposed objective: First, an experiment was conducted with healthy participants wearing a knee exoskeleton to establish an extensive dataset of exoskeleton sensor data during stumble events. This dataset was used to develop a stumble detection algorithm. Next, a previously-generated dataset of stumbles from different participants was used to build a recovery strategy identification algorithm. This algorithm was then tested on the new exoskeleton stumble experiment dataset.

A. Exoskeleton Stumble Experiment

A swing-phase obstacle perturbation stumble experiment was conducted with five healthy adult participants (one female, 4 males; mean age: 28 +/- 4 years; mean height: 1.8 +/- 0.04 m; mean mass: 80 +/- 17 kg) wearing a unilateral knee exoskeleton to collect sensor data with which to develop the stumble detection algorithm and test the recovery strategy identification algorithm. All experimental protocols were approved by the Vanderbilt Institutional Review Board, and all participants gave their written informed consent.

1) Knee Exoskeleton Hardware: The unilateral knee exoskeleton used in these experiments is a standard knee-ankle-foot orthosis (KAFO), diagrammed in Fig. 1. Sensor data from the device were used to develop the detection and identification algorithms. Specifically, a cassette attached to the thigh segment houses a nine-axis IMU and an encoder to measure knee angle. Force-sensing resistors (FSRs) are mounted to the toe and heel of the AFO to detect heel-strike and toe-off. Note that the cassette also included a motor and transmission to actuate the lateral-side knee joint via a pair of Bowden cables, but this feature was not used in the experiments described here.

2) Experimental Protocol: Each participant was introduced to a series of stumbles using a custom obstacle perturbation system [10] (Fig. 2). The protocol was consistent with previous works using this setup [16], [17], [18], namely: the participant, while wearing the knee exoskeleton, walked on a force-instrumented treadmill at 1.1 m/s. After a random number of steps, an obstacle was released onto the treadmill belt at a random percentage of swing phase to unexpectedly obstruct the swing foot, inducing a stumble and requiring a stumble recovery response. Participants listened to white noise, wore noise-cancelling headphones and wore inferior vision-blocking goggles to occlude auditory and visual cues of obstacle release to limit expectation of the perturbation. Additionally, the obstacle delivery apparatus was designed such that the obstacle's entry onto the treadmill belt was imperceptible [10]. Finally, participants performed Serial Sevens (counting backwards by intervals of seven) as a

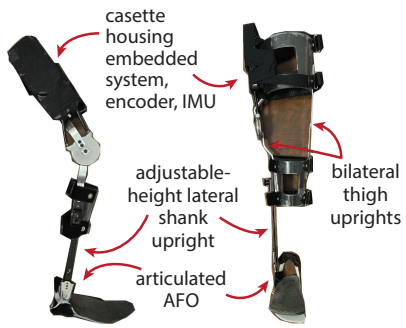

Fig. 1: Knee exoskeleton

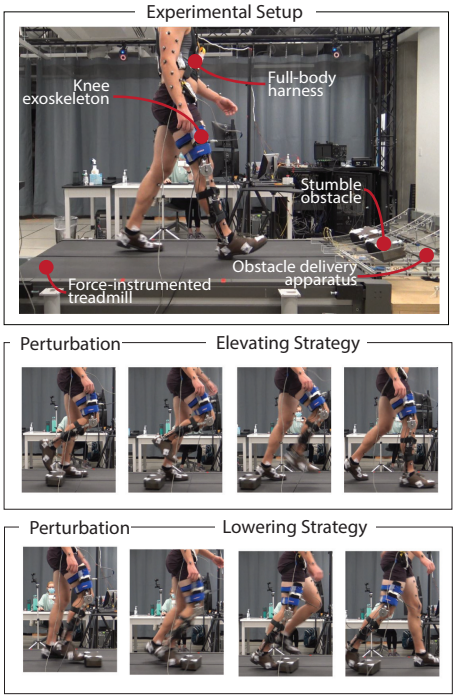

Fig. 2: Stumble experimental setup and responses

cognitive distraction task to further limit expectation and/or anticipation of the perturbation.

3) Data Collection: For each stumble trial (which included steps leading up to the stumble and the stumble itself), raw signals from the exoskeleton knee encoder and thigh IMU were collected via a CAN interface with MATLAB/Simulink at a sampling rate of one kHz. Ground-reaction forces (GRFs) were collected from the split-belt, force-instrumented treadmill (Bertec, Columbus, USA) at one kHz to compute swing percentage of each perturbation. Signal processing is detailed in the subsections discussing each algorithm.

The recovery strategy of each stumble trial was reported as elevating (if the foot cleared the obstacle and landed anterior to it in the same step) or lowering (if the foot lowered posterior to obstacle prior to clearing it), as pictured in Fig. 2. The swing percentage of each stumble was calculated as the time of perturbation relative to the preceding toe-off divided by the average swing time of 20 strides prior to the perturbation.

B. Stumble Detection Algorithm

1) Algorithm Development: IMU data (gyroscope signals in three directions and accelerometer signals in three directions) collected during the exoskeleton stumble experiment (109 stumble trials) were used for algorithm development. Each trial was parsed from the toe-off immediately prior to the perturbation to one second after the toe-off (i.e., post-perturbation), yielding 109 perturbation events. Additionally, the swing phase prior to the perturbed swing phase was parsed from each trial, yielding 109 normal swing phases. Originally, in [16], a singular threshold on thigh acceleration was used for detection. However, when tested on all perturbation events and normal swing phases from this study's dataset, this threshold was not robust across multiple participants; instead, each participant required their own threshold. A threshold approach was explored for the remaining available signals, but no universal threshold(s) could be found that provided accurate detection without false positives. This was consistent with other works which used threshold or outlier-based detection methods [9], [11]. Second, the FFT method from [12] was considered; however, this approach alone also produced many false positives in both the perturbation events (prior to perturbation) and normal swing phases.

Thus, the final detection algorithm (flow chart provided in Fig. 3) involves a combined approach, with thresholds on IMU data in both the frequency and time domain. Specifically, every 10 ms the FFT of the raw thigh acceleration in the y-direction (normal to thigh segment) from the accelerometer is computed for the previous 50 ms. If the magnitude of this FFT at frequencies of 20, 40, 60, or 80 Hz (i.e., frequencies substantially higher than the typical walking frequency of 1-2 Hz) is greater than a threshold, then that instant in time is flagged as a potential perturbation. If flagged, the 10-ms backward difference of the thigh acceleration in the y-direction from the accelerometer (Thigh Jerk Y in Fig. 4) and the 10-ms backward difference of thigh angular velocity from the gyroscope (Thigh Angular Acceleration in Fig. 4) are computed. If both signals exceed certain thresholds in the previous 30 ms, that instant is marked as a perturbation.

2) Outcome Metrics: Detection accuracy was computed as the percentage of perturbation events in which the perturbation was successfully detected. False positive rate was computed as the number of false detections that occurred in total out of the 109 perturbation events and 109 normal swing phases. Finally, detection delay for each of the perturbation events was computed as the time difference between the true perturbation index (identified post-hoc as the first peak in the Thigh Acceleration Y signal) and the perturbation detection

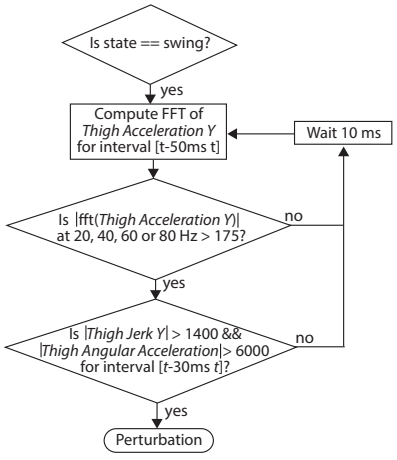

Fig. 3: Stumble detection algorithm flow chart

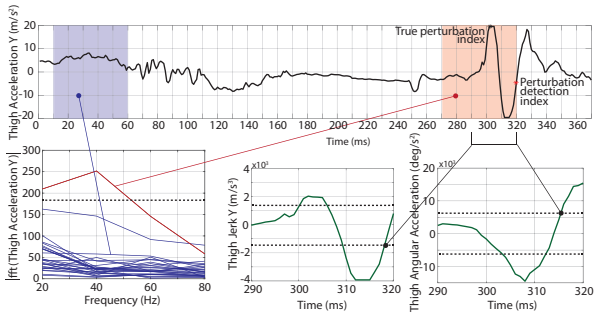

Fig. 4: Stumble detection algorithm implementation on perturbation event. Refer to Fig. 3 for algorithm flow chart.

index (identified with the detection algorithm), indicated in Fig. 4.

C. Recovery Strategy Identification Algorithm

The overarching approach to strategy identification algorithm development for this work was to use a previously collected kinematic dataset of 188 stumbles from seven healthy adults [10] to build a strategy selection model, and then to test this model on the kinematic dataset of 109 stumbles from the exoskeleton stumble experiment described above. Note that both experiments employed the same experimental setup and protocol. A two-stage modelling approach was used, which was previously found to best predict recovery strategies: a first decision between initially elevating and lowering (Stage 1), and, if elevating, a second decision between elevating and delayed lowering (Stage 2) [17]. For this model, only kinematic features easily computed from the sensors onboard the exoskeleton were considered: thigh angle, thigh angular velocity, knee angle, and knee angular velocity.

1) Data Processing & Organization: **Motion Capture Dataset** For the previously collected healthy adult stumble study, lower-limb kinematics were recorded at 200 Hz via an infrared motion capture system and processed with a zero-phase, third-order, Butterworth low-pass filter at a cutoff frequency of 6 Hz. Inverse kinematics were computed using Visual3D (C-Motion, Germantown, USA) to estimate lower-limb kinematics for each trial. The potential inputs (thigh angle, thigh angular velocity, knee angle, and knee angular velocity) were computed at the instant of perturbation, and the recovery strategy was labeled for each stumble. Position inputs (thigh angle, knee angle) were normalized to the value at full extension in the previous step. The trials were split into two datasets for training/validation: the Stage 1 Motion Capture Dataset included all 188 trials labeled as initially elevating or lowering, and the Stage 2 Motion Capture Dataset included the 165 initially elevating trials labeled as elevating or delayed lowering.

Exo Sensor Dataset For the exoskeleton stumble study, lower-limb kinematics were recorded at 1000 Hz via the knee encoder and thigh IMU. Specifically, thigh angle was computed with complementary filter sensor fusion that combines accelerometer and gyroscope measurements with a crossover frequency of 0.1 Hz. Thigh angular velocity was computed via a standard first-order low-pass filter with a cutoff frequency of 30 Hz. Position inputs were normalized to the value at full extension in the previous step. The potential inputs were computed at the true perturbation index, as well as 5, 10 and 15 ms prior to the true perturbation index, and recovery strategy was labeled for each stumble, comprising one Exo Sensor Dataset. Exo Sensor Dataset trials were labeled either elevating (all elevating strategies) or lowering (all lowering and delayed lowering strategies). Because both the delayed lowering strategy and lowering strategy involve ultimately lowering the foot behind the stumble obstacle, and would thus require the same exoskeleton knee assistance, it was not necessary to differentiate between the two in the actual application. Note that these processing steps can be applied in real-time on the exoskeleton, so the testing process represents real-time implementation of the algorithm.

2) Algorithm Development: Initially, the Motion Capture Dataset was explored for insight into which feature subsets best predicted strategy selection. Similar to the approach in [17], [16], a wrapper method with cross-validation by participant and hyperparameter tuning was used to find the total classification accuracy (computed as the average of the classification accuracies of each participant's set of trials) for each of the 15 possible feature subsets shown in Fig. 5. This process was completed for both the Stage 1 and Stage 2 Motion Capture Dataset.

Because no feature subset emerged as substantially best in the cross-validation process for either stage (all performed relatively well, with a classification accuracy range of 88%-97% for Stage 1, and 81%-88% for Stage 2), all 15 feature subsets were considered for model fitting and algorithm testing (i.e., in order to examine to what extent these feature subsets also perform well on the Exo Sensor Dataset) with the following procedure, which is outlined in Fig. 5.

For each feature subset for each stage, the Motion Capture Dataset was fit to a logistic regression model with Ridge regularization (using the hyperparameter that maximized classification accuracy for the corresponding feature set in cross-validation process). The logistic regression equations for Stage 1 (Eq. 1) and Stage 2 (Eq. 2) are given below:

$$P(L) = \frac{1}{1+e^{-(\alpha_0+\alpha_1\gamma+\alpha_2\dot{\gamma}+\alpha_3\theta+\alpha_4\dot{\theta})}} \tag{1}$$

$$P(DL) = \frac{1}{1+e^{-(\beta_0+\beta_1\gamma+\beta_2\dot{\gamma}+\beta_3\theta+\beta_4\dot{\theta})}} \tag{2}$$

Where P(L) is the probability of a lowering strategy vs. an initially elevating strategy, P(DL) is the probability of a delayed lowering strategy vs. an elevating strategy, γ is knee angle, $\dot{\gamma}$ is knee angular velocity, θ is thigh angle, and $\dot{\theta}$ is thigh angular velocity, and α_{0-4} and β_{0-4} are the equation coefficients generated from the model fitting. Note that coefficients have a value of 0 for the features not included in the subset, as indicated in Fig. 5.

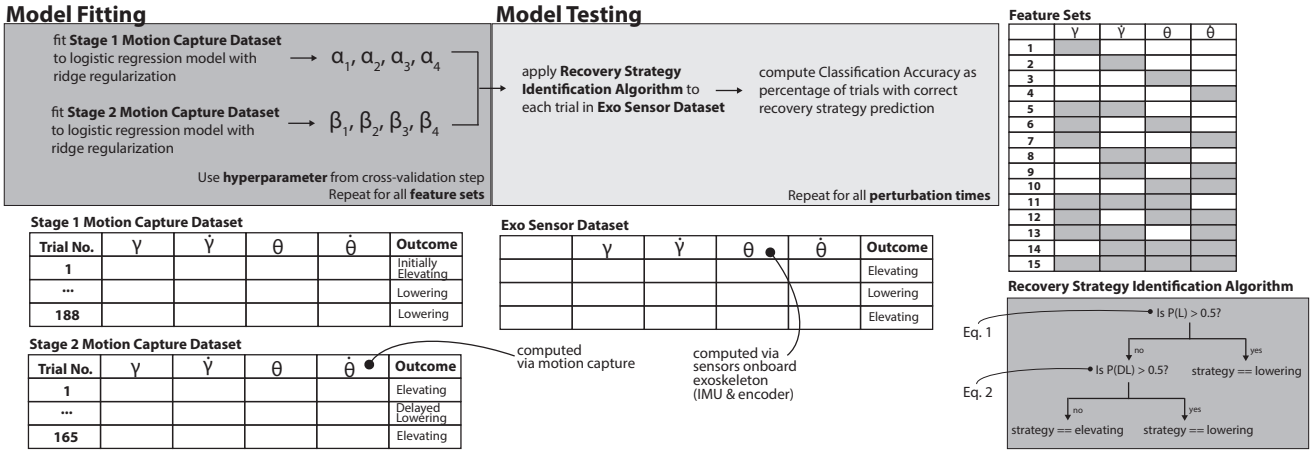

Fig. 5: Recovery strategy identification algorithm development and testing

Fig. 5 diagrams the final recovery strategy identification algorithm: If the probability of lowering (calculated from Eq. 1) is greater than 0.5, then the strategy is predicted to be lowering. If it is less than 0.5, the strategy is predicted to be initially elevating, and Eq.2 (probability of delayed lowering) is computed. If the probability of delayed lowering is greater than 0.5, then the strategy is predicted to be lowering. If it is less than 0.5, the strategy is predicted to be elevating.

For each combination of feature set and stage (15 feature sets for each of two stages = 15^2 combinations), the recovery strategy identification algorithm was applied to each trial in the Exo Sensor Dataset to predict recovery strategy for each trial. This was completed for features computed at the true perturbation index as well as 5, 10, and 15 ms prior. Classification accuracy was computed as the percentage of trials in which recovery strategy was successfully predicted. The combination of Stage 1 feature set, Stage 2 feature set, and perturbation time that produced the highest classification accuracy with the least number of features was chosen as the final algorithm.

3) Outcome Metrics: The logistic regression equation coefficients and perturbation timing used in the final algorithm are reported. Classification results using this final algorithm are also reported, including a confusion matrix, as well as classification accuracy broken down by participant and by swing phase at which the perturbation occurred.

III. Results

A. Stumble Detection Algorithm

Out of 109 perturbation events, the stumble detection algorithm achieved 100% detection accuracy with no false positives. Out of 109 normal swing phases, the stumble detection algorithm yielded no false positives. The average detection delay was 18 +/- 6 ms (range 6-42 ms).

B. Recovery Strategy Identification

The final recovery strategy identification algorithm used the input set computed at 5 ms prior to the true perturbation index. The coefficients from model fitting for each stage are given in Table I. Out of 109 perturbation events, 105 trials were predicted with the correct recovery strategy, yielding a total classification accuracy of 96%. For three of five participants, the classification accuracy for their trials was 100%, and for the remaining two participants it was 86% and 88%. Table II gives a confusion matrix of prediction results, and Fig. 6 provides classification results as a function of swing percentage of perturbation. As shown, all perturbations in early swing (<40%) and all perturbations in late swing (>60%) were predicted correctly, and mid swing perturbations were predicted with 91% classification accuracy.

IV. Discussion

The proposed stumble detection algorithm yielded 100% detection accuracy without false positives, considering 109 perturbation events and 109 normal swing phases. By employing both frequency- and time-domain threshold approaches on the IMU data, this new algorithm builds upon previous works and addresses the previously reported limitations of high false positive rates.

Aside from the improved detection accuracy and false positive rate, this algorithm offers other advantages. First, the algorithm uses a single IMU attached to the thigh, decreasing the number of sensors needed and employing signals more typical of a lower-limb exoskeleton relative to previous works. Furthermore, the detection accuracy using a

TABLE I: Coefficients for equations in recovery strategy identification algorithm

Eq. 1		Eq. 2	
Coefficient	Value	Coefficient	Value
α_0	-5.839	β_0	-2.575e-05
α_1	0.266	β_1	0.083
α_2	0.042	β_2	0
α_3	-0.265	β_3	-0.102
α_4	0	β_4	0

TABLE II: Confusion matrix for recovery strategy identification algorithm results

	Predicted Elevating	Predicted Lowering	Total
Actual Elevating	55	2	57
Actual Lowering	2	50	52
Total	57	52	109

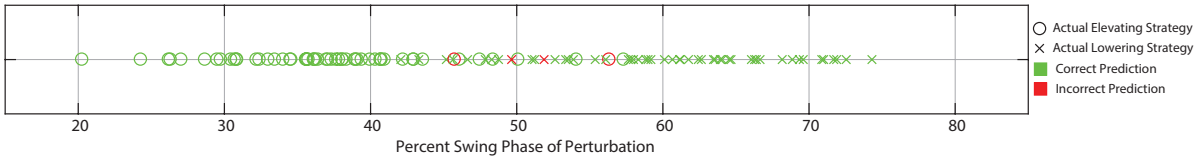

Fig. 6: Recovery strategy identification algorithm results as a function of swing percentage at which the perturbation occurred

thigh IMU (rather than shank or foot) is notable considering this location is two segments removed from the perturbation. Second, this algorithm detects with the fastest response latency compared to other works. The average detection delay out of 109 perturbations was 18 ms, and even the maximum delay (42 ms) is well before the average lower-limb muscle response latencies reported in Schillings et al. 2000 [7]. This short detection delay would allow an assistive to device to react as quickly (or potentially, faster) than the human response, providing the best opportunity for optimal recovery strategy assistance. Finally, the detection and false positive rates were evaluated on 109 stumbles throughout swing phase from five participants, which is the most comprehensive obstacle perturbation stumble dataset used for this application to date.

The stumble recovery strategy identification algorithm predicted recovery strategy with 96% accuracy on a separate test set of 109 stumbles using just three signals from sensor data available in a lower-limb exoskeleton. The algorithm can be easily implemented in real-time on any lower-limb exoskeleton that estimates knee angle, knee angular velocity, and thigh angle (e.g., with a knee encoder and thigh IMU).

In total there were four stumbles incorrectly classified: two elevating strategies (Participant 3) and two lowering strategies (Participant 5). These occurred in the mid swing region where, based on studies of healthy participants (e.g., [7], [19], [20], [10]), either strategy could be selected, and either could be successful. Despite the misclassifications, the algorithm still achieved 91% accuracy in mid swing; note that the best classifier using a simple threshold on swing percentage yields 77% (34/44) accuracy, substantiating the use of real-time, physical quantities as inputs to the model rather than a phase variable [17]. Of note, for three participants the identification algorithm achieved 100% accuracy.

There are several limitations to this work. Regarding the stumble detection algorithm: First, all stumble trials were performed at a single walking speed with one bilateral knee exoskeleton. Thus, detection may potentially require speed-dependent thresholds; likewise, these thresholds may also be influenced by the form factor and weight of the exoskeleton worn, as a heavier exoskeleton may provide a low-pass effect on sensor data that would need to be considered. Second, the exo sensor stumble dataset was used for both detection algorithm development and testing, and as such there is potential for overfitting; however, the authors contend that the thresholds chosen were qualitatively not overly strict and thus should be generalizable, especially considering the nature of the dataset used, which included an extensive number of stumbles throughout swing phase from multiple participants. Thus, the intent for this work was to find thresholds that worked well for this extensive dataset of stumbles, and the authors invite future work to explore the extent to which this detection algorithm extends to more stumbles with new participants, walking speeds, and types/weights of lower-limb exoskeletons. Regarding the recovery strategy identification algorithm: First, an approach to better matching the filtering of the Motion Capture Dataset to the Exo Sensor Dataset may have improved classification accuracy; however the authors posit that 96% accuracy is quite high considering (1) the different measurement modalities, which further shows the algorithm's robustness and generalizability to new data and (2) that strategy selection in mid-swing has been shown to be non-unique. This non-uniqueness raises the question: How important is decision accuracy in this region? In the case of an impaired user, perhaps selection of either strategy in this regime would be effective. In the case of a healthy user, would the decision of the exoskeleton influence the selection of the user? Hopefully future works will help to inform these questions. Second, the intent for this work was to develop and report the recovery strategy identification algorithm that performed best on a new exoskeleton sensor dataset of stumbles after considering various input options; the authors encourage future work that tests this algorithm with new stumble datasets to verify its effectiveness on new data. Finally, the results of this work reflect the efficacy of a stumble detection and recovery strategy identification algorithm for the specific type of perturbation tested: a swing-phase, obstacle perturbation. While falling due to stumbles is a common cause of injury [21], [22], and the test setup best replicates this real-life stumble event compared to other systems [10], research regarding detection and response selection for other types of perturbations (i.e., slips, pushes) are needed and may be a topic for future work.

V. Conclusion

This work develops algorithms for exoskeleton-based, real-time detection of stumble during walking, and importantly also for the real-time selection of stumble recovery strategy, and evaluates these algorithms with a relatively large stumble dataset (i.e., 109 stumbles). These algorithms use minimal sensor data (single thigh IMU for detection, thigh IMU and knee encoder for recovery strategy identification) while detecting a stumble event and identifying appropriate recovery strategy quicker than the human reaction time. This work provides the crucial first step in developing lower-limb assistive devices that are robust to the common event of a trip or stumble, which has the potential to improve safety of these devices and reduce fall risk for fall-prone individuals.

REFERENCES

[1] A. Martínez, C. Durrough, and M. Goldfarb, "A Single-Joint Implementation of Flow Control: Knee Joint Walking Assistance for Individuals With Mobility Impairment," *IEEE Transactions on Neural Systems and Rehabilitation Engineering*, vol. 28, pp. 934–942, Apr. 2020. Conference Name: IEEE Transactions on Neural Systems and Rehabilitation Engineering.

[2] A. Zoss, H. Kazerooni, and A. Chu, "Biomechanical design of the Berkeley lower extremity exoskeleton (BLEEX)," *IEEE/ASME Transactions on Mechatronics*, vol. 11, pp. 128–138, Apr. 2006. Conference Name: IEEE/ASME Transactions on Mechatronics.

[3] D. Pinto-Fernandez, D. Torricelli, M. d. C. Sanchez-Villamanan, F. Aller, K. Mombaur, R. Conti, N. Vitiello, J. C. Moreno, and J. L. Pons, "Performance Evaluation of Lower Limb Exoskeletons: A Systematic Review," *IEEE Transactions on Neural Systems and Rehabilitation Engineering*, vol. 28, pp. 1573–1583, July 2020. Conference Name: IEEE Transactions on Neural Systems and Rehabilitation Engineering.

[4] T. Yan, M. Cempini, C. M. Oddo, and N. Vitiello, "Review of assistive strategies in powered lower-limb orthoses and exoskeletons," *Robotics and Autonomous Systems*, vol. 64, pp. 120–136, Feb. 2015.

[5] D. Shi, W. Zhang, W. Zhang, and X. Ding, "A Review on Lower Limb Rehabilitation Exoskeleton Robots," *Chinese Journal of Mechanical Engineering*, vol. 32, p. 74, Aug. 2019.

[6] M. Grimmer, R. Riener, C. J. Walsh, and A. Seyfarth, "Mobility related physical and functional losses due to aging and disease - a motivation for lower limb exoskeletons," *Journal of NeuroEngineering and Rehabilitation*, vol. 16, p. 2, Jan. 2019.

[7] A. M. Schillings, B. van Wezel, T. Mulder, and J. Duysens, "Muscular responses and movement strategies during stumbling over obstacles," *Journal of Neurophysiology*, vol. 83, pp. 2093–2102, Apr. 2000.

[8] J. J. Eng, D. A. Winter, and A. E. Patla, "Strategies for recovery from a trip in early and late swing during human walking," *Experimental Brain Research*, vol. 102, pp. 339–349, Dec. 1994.

[9] F. Zhang, S. E. D'Andrea, M. J. Nunnery, S. M. Kay, and H. Huang, "Towards Design of a Stumble Detection System for Artificial Legs," *IEEE Transactions on Neural Systems and Rehabilitation Engineering*, vol. 19, pp. 567–577, Oct. 2011.

[10] S. T. King, M. E. Eveld, A. Martínez, K. E. Zelik, and M. Goldfarb, "A novel system for introducing precisely-controlled, unanticipated gait perturbations for the study of stumble recovery," *Journal of NeuroEngineering and Rehabilitation*, vol. 16, p. 69, June 2019.

[11] C. Shirota, A. M. Simon, and T. A. Kuiken, "Recovery strategy identification throughout swing phase using kinematic data from the tripped leg," in *2014 36th Annual International Conference of the IEEE Engineering in Medicine and Biology Society*, pp. 6199–6202, Aug. 2014.

[12] B. E. Lawson, H. Atakan Varol, F. Sup, and M. Goldfarb, "Stumble detection and classification for an intelligent transfemoral prosthesis," *Conference proceedings: ... Annual International Conference of the IEEE Engineering in Medicine and Biology Society. IEEE Engineering in Medicine and Biology Society. Annual Conference*, vol. 2010, pp. 511–514, 2010.

[13] V. Monaco, P. Tropea, F. Aprigliano, D. Martelli, A. Parri, M. Cortese, R. Molino-Lova, N. Vitiello, and S. Micera, "An ecologically-controlled exoskeleton can improve balance recovery after slippage," *Scientific Reports*, vol. 7, p. 46721, May 2017. Number: 1 Publisher: Nature Publishing Group.

[14] D. den Hartog, "The Stumblemeter: Design and validation of a system that detects and classifies human stumbling during gait," 2021.

[15] N. Hajj Chehade, P. Ozisik, J. Gomez, F. Ramos, and G. Pottie, "Detecting stumbles with a single accelerometer," in *2012 Annual International Conference of the IEEE Engineering in Medicine and Biology Society*, pp. 6681–6686, Aug. 2012. ISSN: 1558-4615.

[16] M. Eveld, S. King, K. Zelik, and M. Goldfarb, "Design and implementation of a stumble recovery controller for a knee exoskeleton," in *2021 IEEE/RSJ International Conference on Intelligent Robots and Systems (IROS)*, pp. 6196–6203, Sept. 2021. ISSN: 2153-0866.

[17] M. E. Eveld, S. T. King, L. G. Vailati, K. E. Zelik, and M. Goldfarb, "On the Basis for Stumble Recovery Strategy Selection in Healthy Adults," *Journal of Biomechanical Engineering*, Feb. 2021.

[18] M. E. Eveld, S. T. King, K. E. Zelik, and M. Goldfarb, "Factors leading to falls in transfemoral prosthesis users: A case series of sound-side stumble recovery responses," *Journal of NeuroEngineering and Rehabilitation*, 2022.

[19] A. F. Cordero, H. J. F. M. Koopman, and F. C. T. van der Helm, "Mechanical model of the recovery from stumbling," *Biological Cybernetics*, vol. 91, pp. 212–220, Oct. 2004.

[20] C. Shirota, A. M. Simon, and T. A. Kuiken, "Trip recovery strategies following perturbations of variable duration," *Journal of Biomechanics*, vol. 47, pp. 2679–2684, Aug. 2014.

[21] M. E. Tinetti, D. I. Baker, G. McAvay, E. B. Claus, P. Garrett, M. Gottschalk, M. L. Koch, K. Trainor, and R. I. Horwitz, "A Multifactorial Intervention to Reduce the Risk of Falling among Elderly People Living in the Community," *New England Journal of Medicine*, vol. 331, pp. 821–827, Sept. 1994. Publisher: Massachusetts Medical Society _eprint: https://doi.org/10.1056/NEJM199409293311301.

[22] T. Leamon and P. Murphy, "Occupational Slips and Falls: More than a Trivial Problem," *Ergonomics*, vol. 38, pp. 487–98, Apr. 1995.